JCB Article

Sequential exocytosis of insulin granules is associated with redistribution of SNAP25

Noriko Takahashi,[1,2] Hiroyasu Hatakeyama,[1] Haruo Okado,[3] Akiko Miwa,[3] Takuya Kishimoto,[1] Tatsuya Kojima,[1] Teruo Abe,[4] and Haruo Kasai[1]

[1]Department of Cell Physiology, National Institute for Physiological Sciences, Graduate University of Advanced Studies, Myodaiji, Okazaki 444-8585, Japan
[2]Precursory Research for Embryonic Science and Technology, Japan Science and Technology Agency, Kawaguchi, Saitama 332-0012, Japan
[3]Department of Molecular Physiology, Tokyo Metropolitan Institute for Neuroscience, Fuchu, Tokyo 183-8526, Japan
[4]Department of Cellular Neurobiology, Brain Research Institute, University of Niigata, Niigata, Niigata 951-8585, Japan

We have investigated sequential exocytosis in β cells of intact pancreatic islets with the use of two-photon excitation imaging of a polar fluorescent tracer, sulforhodamine B, and a fusion protein comprising enhanced cyan fluorescent protein (ECFP) and the SNARE protein SNAP25 (synaptosome-associated protein of 25 kD) transfected with an adenoviral vector. Sequential exocytosis was found to account for <10% of exocytic events in β cells stimulated either with glucose under various conditions or by photolysis of a caged-Ca^{2+} compound. Multigranular exocytosis, in which granule-to-granule fusion occurs before exocytosis, was rarely found. We detected redistribution of ECFP-SNAP25 from the plasma membrane into the membrane of the fused granule occurred in a large proportion (54%) of sequential exocytic events but in only a small fraction (5%) of solitary fusion events. Removal of cholesterol in the plasma membrane by methyl-β-cyclodextrin facilitated both redistribution of ECFP-SNAP25 and sequential exocytosis by threefold. These observations support the hypothesis that SNAP25 is a plasma membrane factor that is responsible for sequential exocytosis.

Introduction

Secretory cells often exhibit exocytic events that involve more than one vesicle (Ichikawa, 1965; Rohlich et al., 1971; Douglas, 1974; Orci and Malaisse, 1980; Dvorak et al., 1981; Tai and Spry, 1981) and have been referred to as "compound exocytosis." However, these events include two distinct phenomena, sequential and multigranular exocytosis (Alvarez de Toledo and Fernandez, 1990; Scepek and Lindau, 1993; Cochilla et al., 2000; Nemoto et al., 2001). In sequential exocytosis, vesicles fuse selectively with other vesicles that have already fused with the plasma membrane (Ichikawa, 1965; Rohlich et al., 1971; Cochilla et al., 2000; Nemoto et al., 2001). In contrast, in multigranular exocytosis, multiple vesicles fuse with each other before exocytosis (Dvorak et al., 1981; Tai and Spry, 1981; Alvarez de Toledo and Fernandez, 1990; Scepek and Lindau, 1993). Quantitation of these two types of compound exocytosis has been difficult with classical methodologies. For example, sequential exocytosis cannot be detected by measurement of capacitance (Alvarez de Toledo and Fernandez, 1990; Scepek and Lindau, 1993) or by amperometry because these techniques lack the necessary spatial resolution; it is also not amenable to analysis with conventional microscopes because they are not suited for evaluation of events that occur deep inside a cell (Oheim et al., 1999; Cochilla et al., 2000; Zenisek et al., 2002). Electron microscopy also cannot readily distinguish sequential from multigranular exocytosis (Rohlich et al., 1971; Cochilla et al., 2000).

The dynamics of sequential exocytosis in pancreatic acini have been revealed by two-photon excitation microscopy (Nemoto et al., 2001). In this approach, the secretory glands are placed in a solution containing a polar fluorescent tracer, and the individual exocytic events are detected by

The online version of this article includes supplemental material.

Address correspondence to H. Kasai, Dept. of Cell Physiology, National Institute for Physiological Sciences, Graduate University of Advanced Studies, Myodaiji, Okazaki 444-8585, Japan. Tel.: 81-564-55-7831. Fax: 81-564-53-7341. email: hkasai@nips.ac.jp

Keywords: diabetes; two-photon imaging; secretion; SNARE; pancreatic islet

Abbreviations used in this paper: AM, acetoxymethyl ester; AU, arbitrary unit; $[Ca^{2+}]_i$, cytosolic-free Ca^{2+} concentration; NP-EGTA, *o*-nitrophenyl–EGTA; ROI, region of interest; SNAP25, synaptosome-associated protein of 25 kD; SRB, sulforhodamine B.

The Journal of Cell Biology, Volume 165, Number 2, April 26, 2004 255–262
http://www.jcb.org/cgi/doi/10.1083/jcb.200312033

The Journal of Cell Biology

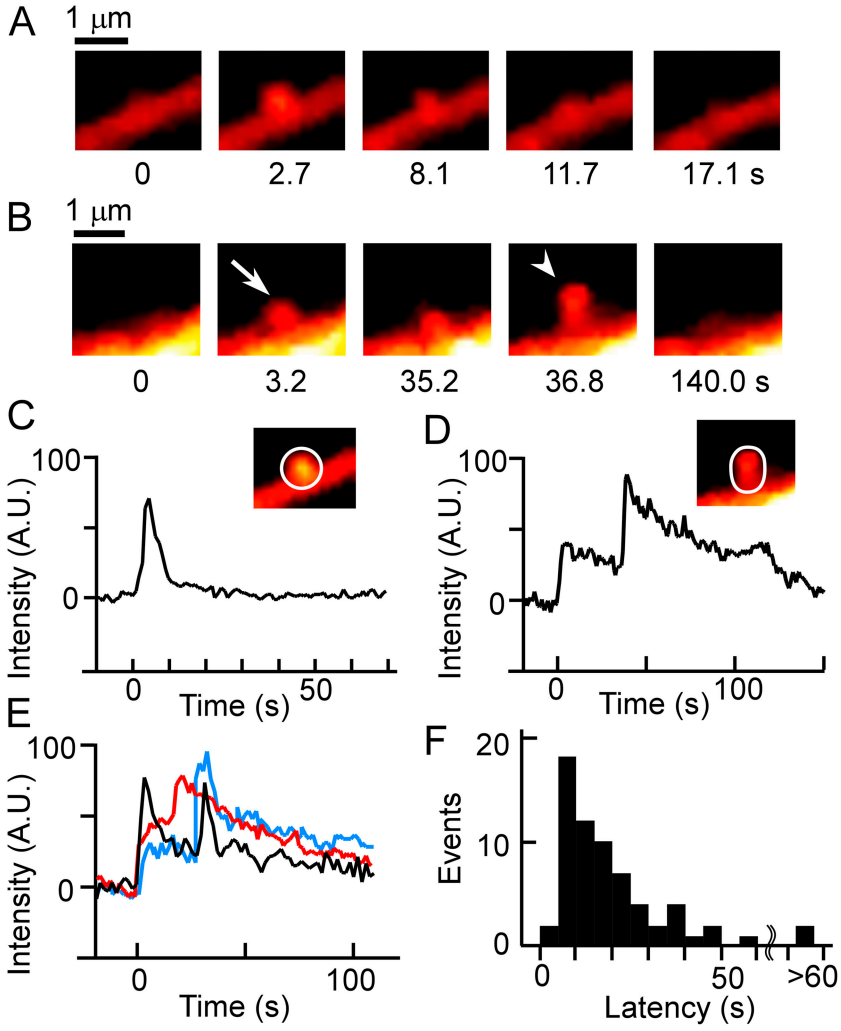

Figure 1. **Insulin exocytic events revealed by two-photon excitation imaging in mouse pancreatic islets.** Islets were superfused with a solution containing 0.7 mM SRB and were stimulated by exposure to 20 mM glucose. (A and B) En face views of insulin exocytic events. The numbers below each panel represent time after the onset of exocytosis. The Ω-shaped profile of the primary exocytic granule (arrow) in B becomes the target for a secondary exocytic event (arrowhead); the two granules finally flattened out within the plasma membrane. (C and D) Changes in fluorescence intensity (AU, arbitrary unit) within the ROIs (white outlines in the insets) containing the exocytic granules shown in A and B, respectively. The fluorescence value before exocytosis was set to zero. (E) Three additional examples of sequential exocytic events. (F) Latency histogram for the delay between the onsets of the primary and secondary events during sequential exocytosis.

the appearance of Ω-shaped fluorescent profiles. We have found that the inner filter effect of bright fluid-phase tracers with large extinction coefficients, such as sulforhodamine B (SRB; Takahashi et al., 2002), is absent in two-photon excitation imaging, so that we can use high concentrations of polar tracers to image individual exocytic events. Sequential exocytosis, which proceeds deep within the cytoplasm, is apparent as beadlike strands of exocytosed vesicles. The rapid appearance of a large fluorescent profile corresponding to multigranular exocytosis was rarely detected in pancreatic acini (Nemoto et al., 2001). Two-photon excitation imaging with an extracellular dye is thus a reliable method with which to quantify the two types of compound exocytosis in intact tissue.

This method has previously been applied to pancreatic islets to monitor the exocytosis of individual insulin granules (Takahashi et al., 2002). We have now systematically investigated the possible occurrence of sequential and multigranular exocytosis in β cells of intact islets as well as performed real-time measurements of the redistribution of a SNARE protein (Wei et al., 2000), SNAP25 (synaptosome-associated protein of 25 kD), during individual sequential exocytic events, taking advantage of the simultaneous multicolor imaging facility of the two-photon microscope (Nemoto et al., 2001;Takahashi et al., 2002).

Results

Quantitation of sequential exocytosis in β cells

Individual exocytic events in β cells were visualized by two-photon excitation microscopic analysis of intact mouse pancreatic islets superfused with a solution containing the polar fluorescent tracer SRB (see Fig. 3 A). The islets were stimulated by exposure to 20 mM glucose. As previously described (Nemoto et al., 2001;Takahashi et al., 2002), we detected the abrupt appearance of small fluorescent spots at the plasma membrane that reflect individual insulin exocytic events (Fig. 1 A). Most of these fluorescent spots rapidly decayed as a result of flattening of the granule membrane into the plasma membrane (Fig. 1, A and C; Takahashi et al., 2002). We examined the occurrence of sequential exocytosis in en face views of exocytic events (Fig. 1 A) that occurred toward regions of the plasma membrane that were both almost orthogonal to the focal plane and distant from out-of-focus regions of the membrane.

Exocytosed granules became a target for the subsequent fusion of adjacent granules deeper within the cytoplasm (Fig. 1, B and D; and Video 1, available at http://www.jcb.org/cgi/content/full/jcb.200312033/DC1) in only a small proportion (2.6%) of events (Table I). The maximal fluorescence intensity of secondary exocytic events expressed

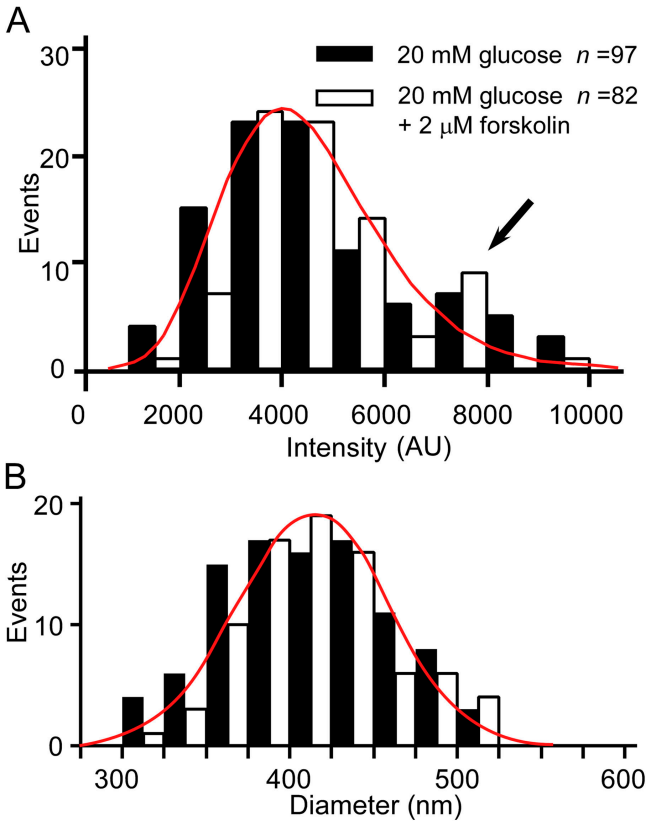

Figure 2. **Distributions of the fluorescence intensity of individual exocytic events and of the diameter of exocytosed granules.** (A) Distributions of the increase in fluorescence intensity associated with individual exocytic events in islets stimulated with 20 mM glucose (black bars) or with 20 mM glucose and 2 μM forskolin (white bars). The mean intensities were 4,671 ± 1,950 AU (n = 97) and 4,680 ± 1,530 AU (± SD, n = 82), respectively. The arrow indicates an apparent excess of large components. (B) Distributions of granule diameter estimated from the fluorescence intensity distributions shown in A. The smooth lines represented the Gaussian distribution with a mean and SD of 0.42 and 0.05 μm, respectively.

relative to that of the corresponding primary event was 1.07 ± 0.54 (mean ± SD, n = 11), supporting that the secondary events also reflected exocytosis of insulin granules. Such secondary fused granules were seldom the target for further exocytosis, instead, they eventually flattened out within the plasma membrane (Fig. 1, A and C). Thus, sequential exocytosis was found to occur in β cells but at a relatively low frequency.

Next, we assessed the proportion of all exocytic events attributable to sequential exocytosis, given that en face events represented only 5–15% of all events. A definition of sequential exocytosis as the detection of two successive exocytic events in which the vesicles are in apparent contact with a center-to-center distance of <0.5 μm (Fig. 1 B) yielded a value of 1.9% for the contribution of sequential exocytosis to total exocytosis (Table I). This value was not significantly different ($P > 0.1$) from that estimated from the en face events, which is consistent with the observations that there do not appear to be hot spots of exocytosis in β cells (Takahashi et al., 2002) and that exocytic events are widely separated in the plasma membrane (0.017 events μm^{-2} min^{-1}; see Materials and methods), with simultaneous events within a distance of <0.5 μm being predicted to occur at a frequency of 0.18–0.33%/min. Moreover, 82% (53/65) of secondary exocytic events occurred within 30 s after the onset of the primary event (Fig. 1, E and F), providing further support for a causal relation between the primary and secondary exocytic events.

Effects of cAMP, PMA, and temperature on sequential exocytosis

Exposure of islets either to 2 μM forskolin, which increases the intracellular concentration of cAMP, or to 400 nM PMA, which activates protein kinase C, in the presence of 20 mM glucose resulted in a two- to fourfold increase in the frequency of insulin exocytosis compared with that apparent in the presence of 20 mM glucose alone (Table I). However,

Table I. **Proportion of all exocytic events attributable to sequential exocytosis under various experimental conditions**

Condition	Exocytosis	Proportion of sequential exocytosis	
		En face events[a]	Total events[a]
	events cell^{-1} min^{-1}	*%*	*%*
Acinar cells			
100 pM cholecystokinin		>50	>50
Islet cells			
20 mM glucose	11.2	2.6 (77)	1.9 (693)
20 mM glucose + 2 μM forskolin	26.7	2.4 (84)	1.0 (964)
20 mM glucose + 400 nM PMA	44.8	2.0 (51)	2.3 (651)
20 mM glucose (35°C)	21.5	1.9 (92)	3.6 (388)
20 mM glucose + 2 μM forskolin (35°C)	45		4.5 (224)
20 mM glucose + 400 nM PMA (35°C)	40		3.9 (102)
60 mM KCl	18.8		1.3 (521)
100 μM acetylcholine	6.8		1.2 (243)
NP-EGTA	48.6	2.4 (83)	3.3 (563)
20 mM glucose + 2 μM forskolin (15 mM methyl-β-cyclodextrin)	4.8		8.9 (416)

The data for acinar cells are from Nemoto et al. (2001). The contribution of sequential exocytosis to total exocytic events was significantly different from the value (2.6%) for en face events during glucose stimulation only in methyl-β-cyclodextrin–treated preparations (χ^2 test, $P < 0.01$).
[a]Numbers in parentheses refer to the number of events analyzed.

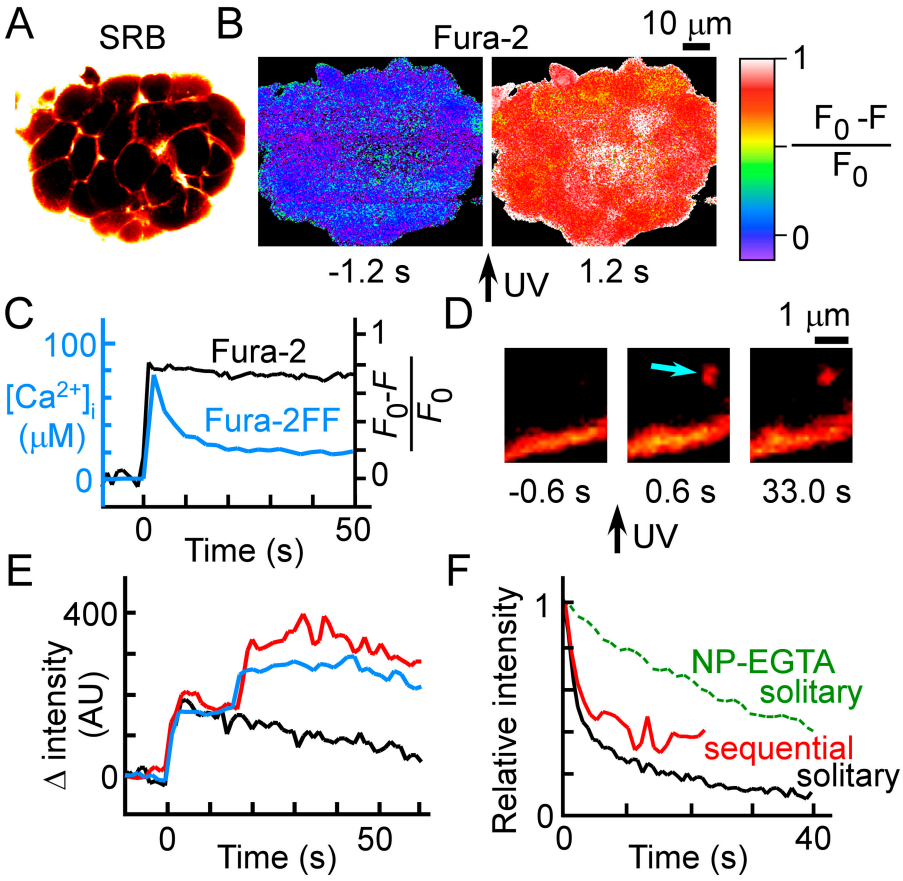

Figure 3. **Exocytic events triggered by photolysis of a caged-Ca^{2+} compound.** (A) SRB fluorescence image of an islet that had been preloaded with NP-EGTA and fura-2. (B) Fura-2 (Ca^{2+}) images obtained 1.2 s before and after UV irradiation of the islet shown in A. (C) Representative time courses of normalized fura-2 fluorescence (black) and of $[Ca^{2+}]_i$ estimated with fura-2FF (blue). Fura-2 fluorescence (F) was normalized by the resting fluorescence (F_0), and the trace shown is for the islet in B. (D) Exocytic event (arrow) triggered by UV photolysis of NP-EGTA. Ω Profiles often persisted for tens of seconds. (E) Two examples of time courses of sequential exocytosis (blue and red) and an example of that of solitary exocytosis (black) triggered by photolysis of NP-EGTA. The traces were aligned at the onset of exocytosis. (F) Time courses of the decay of SRB fluorescence associated with exocytic events induced by 20 mM glucose (black and red) or by photolysis of NP-EGTA (green). The traces are averages of >10 exocytic events, which were aligned at the peak of SRB fluorescence and normalized by the peak intensity. The data correspond to solitary events (black and green) or to the primary event of sequential exocytosis (red).

the proportion of sequential exocytic events was unaffected by either of these agents (Table I). The contribution of sequential exocytosis to total exocytosis also did not differ between islets stimulated with 20 mM glucose and those stimulated either with acetylcholine or with a high concentration of K^+ (Table I).

Although sequential exocytosis is frequent in the exocrine pancreas even at room temperature (Table I), we tested the possibility that its frequency might be increased in β cells at higher temperatures (33–35°C). Although the frequency of glucose-induced exocytosis was approximately doubled by increasing the temperature, the proportion of sequential exocytic events was not significantly altered ($P > 0.1$, Table I). Indeed, the contribution of sequential exocytosis was not significantly increased even in the presence of 2 μM forskolin or 400 nM PMA at 33–35°C (Table I).

Quantitation of multigranular exocytosis

To evaluate the possible occurrence of multigranular exocytosis in β cells, we determined the distribution of the fluorescence intensity of individual exocytic events (Fig. 2 A). The distribution was skewed, with an excess of large components. However, the diameters of granules estimated from the fluorescence intensities (see Materials and methods; Fig. 2 B) fit well with a Gaussian distribution (Fig. 2 B, red line), which is consistent with previous ultrastructural data (Dean, 1973) and can account for the skewed distribution in the volume of granules (Fig. 2 A, red line; Bekkers et al., 1990). The distributions of fluorescence intensity and granule diameter were not affected by exposure of islets to forskolin (Fig. 2) or PMA (not depicted) in the presence of 20 mM glucose. The intensity distribution was also similar at 33–35°C (unpublished data). Thus, these data indicate the occurrence of little if any multigranular exocytosis in β cells.

Insulin exocytosis evoked by photolysis of a caged-Ca^{2+} compound

The small contribution of sequential exocytosis to total exocytosis in β cells might have been attributable to the relatively small increase in cytosolic-free Ca^{2+} concentration ($[Ca^{2+}]_i$; <5 μM; Bokvist et al., 1995) apparent during stimulated exocytosis in these cells compared with that observed in pancreatic acinar cells (>10 μM; Ito et al., 1997; Nemoto et al., 2001). To test this possibility, we triggered insulin exocytosis with a large and rapid increase in $[Ca^{2+}]_i$ induced by photolysis of the caged-Ca^{2+} compound *o*-nitrophenyl–EGTA (NP-EGTA). We loaded β cells with NP-EGTA and a Ca^{2+} indicator before exposure of the islets to SRB (Fig. 3 A). The islets were irradiated with ultraviolet light to induce the increase in $[Ca^{2+}]_i$ (Fig. 3, B–D). The peak increase in $[Ca^{2+}]_i$ was >20 μM. We examined mostly the outer second and third layers of cells within each islet, which consist predominantly of β cells. The fraction of exocytic events that appeared between 0 to 1 s after the onset of the increase in $[Ca^{2+}]_i$ is only 12.4 ± 6.8% (mean ± SD, n = 921 events, 11 islets) of the total events recorded between 0 and 10 s, which is in accordance with the results using amperometry (Takahashi et al., 1997, 1999).

Although we detected sequential exocytosis (Fig. 3 E), its contribution to total exocytosis was not significantly greater than that apparent during glucose stimulation (Table I). The distribution of fluorescence intensity again also revealed no multigranular exocytosis (unpublished data). Exocytosed granules tended to flatten rapidly during glucose stimulation of β cells (Fig. 3 F; Takahashi et al., 2002), which might be expected to impede sequential exocytosis. However, we found that the Ω profiles were stable during stimulation of β cells with the caged-Ca^{2+} compound (Fig. 3, D and F); the fusion pores of most of these fused granules remained open, as revealed by the observation that SRB within the granules could be washed out after removal of the tracer from the bathing solution (not depicted). The Ω profiles of solitary fusion events during stimulation by photolysis of the caged-Ca^{2+} compound were also more stable than those of the primary fusion events of sequential exocytosis observed during glucose stimulation (Fig. 3 F), suggesting that the instability of Ω profiles cannot account for the rarity of sequential exocytosis apparent in β cells during glucose stimulation.

Redistribution of SNAP25 associated with sequential exocytosis

It has been proposed that sequential exocytosis is facilitated by the lateral diffusion of target SNARE proteins from the plasma membrane into the membrane of the fused granule (Nemoto et al., 2001). To test this hypothesis, we transfected islets with an adenoviral vector encoding an ECFP-SNAP25 fusion protein (Fig. 4 B). The ECFP-SNAP25 protein was localized predominantly to the plasma membrane, which is consistent with the localization of the endogenous SNARE protein (Jacobsson et al., 1994). Expression of ECFP-SNAP25 did not affect either the frequency of exocytic events induced by 20 mM glucose in the presence of 2 μM forskolin (26.1 ± 7.7 events $cell^{-1}$ min^{-1}, $n = 7$) or the proportion of sequential exocytosis (1.3%, $n = 312$, $P > 0.1$).

We measured the time course of ECFP-SNAP25 fluorescence at the site of primary exocytosis by simultaneous two-photon imaging of SRB (Fig. 4 A) and ECFP-SNAP25 (Fig. 4 B). During sequential exocytic events (Fig. 4 C, arrowhead), substantial increases in ECFP-SNAP25 fluorescence were detected at the site of primary exocytic event (Fig. 4, C–E), as most clearly seen in the difference images (Fig. 4 F). Such redistribution of ECFP-SNAP25 was rarely detected for solitary events, even when the lifetime of the Ω profile was relatively long (Fig. 4 G), whereas it was quite often detected in the sequential exocytic events (Fig. 4, E and H).

We quantified the increase in ECFP-SNAP25 fluorescence apparent 5–20 s after the onset of the SRB signal for sequential exocytic events, solitary fusion events, and arbitrary regions of the plasma membrane without exocytosis, respectively (Fig. 5 A). The distributions of the increases in ECFP-SNAP25 fluorescence (Fig. 5 A, inset) differed significantly between sequential and solitary exocytic events (Smirnov test, $P < 0.01$) and between solitary events and arbitrary regions ($P < 0.05$). No increase in fluorescence larger than 15 arbitrary units (AU) was detected in arbitrary regions (Fig. 5 A). If we set the threshold level for significant redistribution at 15 AU, the redistribution was significant in

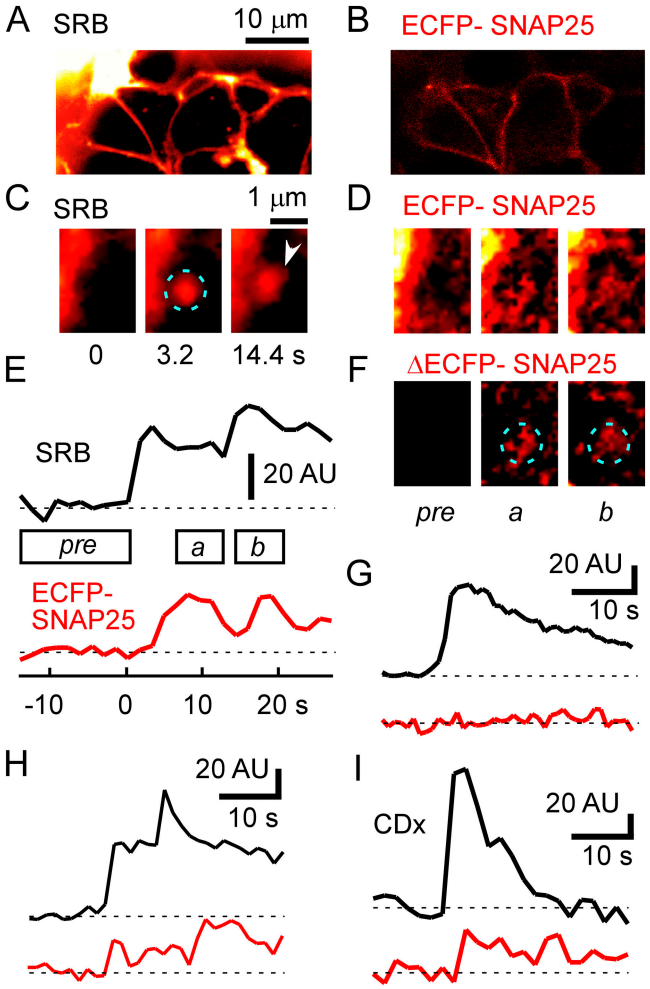

Figure 4. **Redistribution of SNAP25 during sequential exocytosis.** SRB (A) and ECFP-SNAP25 (B) fluorescence images of an islet. The islet was transfected with an adenoviral vector encoding ECFP-SNAP25 and immersed in a solution containing polar tracers, SRB. Simultaneous measurement of SRB (C) and ECFP-SNAP25 (D) fluorescence during a sequential exocytic event. The number below each image in C represents the time after the onset of exocytosis. The blue dashed circle represents the ROI. Each image in D was obtained by averaging 5–10 images in the three time periods shown in E. (E) Time courses of fluorescence of SRB (black) and ECFP-SNAP25 (red) in the ROI shown in C. Open horizontal bars represent time periods between −14.4 and 0 s after the onset of exocytosis (pre), between 6.4 and 12.8 s (a), and between 14.4 and 20.8 s (b). Dashed horizontal lines show baseline fluorescence levels. (F) Difference images obtained by subtracting image pre from three images in D. (G–I) Time courses of fluorescence for another example of sequential exocytosis (H), and examples of solitary exocytic events in a control cell (G) and in a cell treated with 15 mM methyl-β-cyclodextrin for 30 min (I).

54% of sequential exocytic events ($n = 36$) but in only 5% of solitary exocytic events ($n = 354$; χ^2 test, $P < 0.01$). The mean fluorescence increase for the events with significant redistribution was larger in sequential exocytic events (mean ± SD = 25.6 ± 10.7 AU, $n = 14$, $P < 0.01$) than in solitary exocytic events (20.8 ± 6.3 AU, $n = 18$). The mean baseline fluorescence was 20.6 ± 12.5 AU ($n = 17$).

The ECFP-SNAP25 signal always began after the onset of exocytosis (Fig. 5 B, mean ± SD = 6.3 ± 6.1 s, $n = 19$),

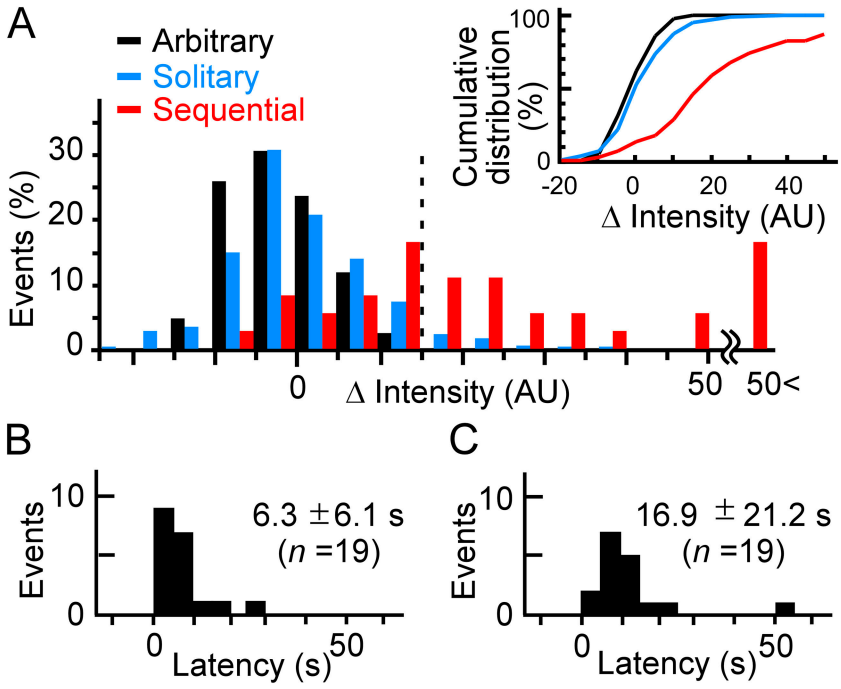

Figure 5. **Amplitudes and latencies of the redistribution of ECFP-SNAP25.** (A) Histograms for the maximal increase in fluorescence intensity of ECFP-SNAP25 between 5 and 20 s after primary exocytosis for solitary events (blue), the primary events of sequential exocytosis (red), and arbitrary regions of the plasma membrane (black). The vertical dashed line represents the noise level. (inset) Cumulative intensity plots for the three histograms. (B and C) Latency histograms for the delay between the onset of exocytosis (the primary events of sequential exocytosis) and that of the ECFP-SNAP25 signal (B) and between the onset of the ECFP-SNAP25 signal and the secondary event of sequential exocytosis (C). Values shown above the plots are means ± SD.

mostly within 5 s (mean ± SD = 4.0 ± 9.4 s, n =19) after the peak of SRB fluorescence (Fig. 4, E and H), which reflects the opening of a fusion pore with a diameter of 12 nm (Takahashi et al., 2002). This observation suggests that SNAP25 diffuses laterally along a large fusion pore. The secondary fusion events occurred 16.9 ± 21.2 s (Fig. 5 C, n = 19) and 14.1 ± 11.9 s (n =19; not depicted) after the onset of the ECFP-SNAP25 signal during stimulation with glucose or by photolysis of NP-EGTA, respectively, suggesting that the interaction between the target and vesicle SNARE proteins occurred within this period.

Effects of cyclodextrin treatment

To investigate whether or not cholesterol-dependent lipid rafts were involved in regulating lateral diffusion of t-SNARE (Chamberlain et al., 2001), we treated islet preparations with methyl-β-cyclodextrin (15 mM in Sol A, 30–60 min). Such treatment was known to deplete cholesterol selectively from membrane (<40%), leaving phospholipid unaffected (Lang et al., 2001), and to induce dispersion of the clusters of the intrinsic plasma membrane-associated SNAREs in PC12 cells (Lang et al., 2001). When we stimulated cyclodextrin-treated islets with 20 mM glucose and 2 μM forskolin, the frequency of insulin exocytosis was reduced to ∼20% (4.8 events cell^{-1} min^{-1}, n = 4, Table I), as reported in PC12 cells (Lang et al., 2001). However, the proportion of sequential exocytosis was increased by 3.7-fold (Table I, 8.9%, n = 416). In addition, significant redistribution of ECFP-SNAP25 fluorescence (threshold level at 15 AU, Fig. 4 I) was more frequently observed by 2.7-fold (14.9%, n = 201) than in untreated control cases (5.8%, n = 361).

Treatment with methyl-β-cyclodextrin also reduced the delay between the onset of exocytosis and that of the ECFP-SNAP25 signal from 8.2 ± 7.2 s (n =12) to 2.4 ± 2.5 s (n = 19, P < 0.01) in solitary events, and from 6.3 ± 6.1 s (n = 19) to 3.5 ± 2.3 s (n = 4, P > 0.05) in sequential events. The time during which SNAP-25 signal reaches the maximal values was not affected by cyclodextrin (unpublished data). The mean fluorescence increase for the events with significant redistribution was not significantly different from control in solitary events (21.8 ± 8.1 AU, n = 30, P > 0.05), and in sequential events (26.5 ± 16.9 AU, n = 7, P > 0.05).

Discussion

Although sequential exocytosis is operative in the β cells of intact pancreatic islets, we have demonstrated that it occurred with only a low frequency under all of the experimental conditions examined. The sequential exocytosis of insulin granules was previously suggested to occur by an ultrastructural study (Orci and Malaisse, 1980) and by confocal imaging (Leung et al., 2002). Although the occurrence of multigranular exocytosis in β cells was also suggested by amperometric measurements (Bokvist et al., 2000) and confocal imaging (Leung et al., 2002), our two-photon imaging data indicate that this is not the case. In contrast to β cells, >50% of exocytic events involving zymogen granules in pancreatic acinar cells occur in a sequential manner (Nemoto et al., 2001). Sequential exocytosis also appears to take place frequently in pituitary lactotrophs (Cochilla et al., 2000) and mast cells (Rohlich et al., 1971; Alvarez de Toledo and Fernandez, 1990), whereas multigranular exocytosis prevails in leukocytes (Dvorak et al., 1981; Tai and Spry, 1981; Scepek and Lindau, 1993; Hafez et al., 2003; Hartmann et al., 2003). Sequential exocytosis and multigranular exocytosis appear to be regulated differentially in different secretory cell types. The relative infrequency of sequential exocytosis in β cells likely reflects an intrinsic property of the fusion machinery, given that the proportion of sequential exocytic events was unaffected by the strength of the stimulus or by the stability of the Ω profile.

Our data support the hypothesis that redistribution of a target SNARE protein from the plasma membrane into the membrane of a fused granule after opening of the fusion pore plays an important role in sequential exocytosis in β cells, as has been proposed for pancreatic acinar cells (Nemoto et al., 2001). Thus, sequential exocytosis in β cells was preferentially associated with a redistribution of ECFP-SNAP25 apparent after opening of the fusion pore. Furthermore, the cyclodextrin treatment, which enhanced redistribution of SNAP25 by 2.6-fold, increased the proportion of sequential exocytosis by 3.7-fold. The observation that 46% of sequential exocytic events were not associated with such redistribution might be attributable to the small signal/noise ratio of ECFP-SNAP25 fluorescence or to the presence of endogenous SNAP25. Conversely, the redistribution of ECFP-SNAP25 was associated with only 5% of solitary exocytic events, and the extent of the redistribution in these instances was smaller than that apparent for sequential events. This result suggests that sequential exocytosis is regulated by the redistribution of SNAP25 in a concentration-dependent manner. Infrequency (∼5%) or inhibition of the lateral diffusion of SNAP25 might be the major factor limiting the frequency of sequential exocytosis in pancreatic β cells. In mast cells, where massive sequential exocytosis occurs (Alvarez de Toledo and Fernandez, 1990), substantial relocation of SNAP23 was found after exocytosis (Guo et al., 1998). Such relocation might, at least partly, reflect redistribution of SNAP23 into granules as in β cells.

We found that the depletion of cholesterol by methyl-β-cyclodextrin from the plasma membrane increased the frequency of redistribution of ECFP-SNAP25 and shortened the latency between the onset of primary exocytosis and that of redistribution of ECFP-SNAP25. Cholesterol binds directly to syntaxin 1A (Lang et al., 2001), and SNAP25 forms a heterodimer with syntaxin 1A (Chamberlain et al., 2001). Therefore, the depletion of cholesterol may facilitate the diffusion of SNAP25 along the plasma membrane and thereby enhances redistribution of SNAP25 into fused granules. Alternatively, cholesterol depletion may alter properties of the fusion pore so that diffusion of SNAP25 along fusion pore is facilitated. The more frequent and rapid redistribution of SNAP25 can account for the increase in the proportion of sequential exocytosis, but only to 8.9%, and the major molecular mechanisms of the inhibition of sequential exocytosis remain to be clarified.

The suppression of sequential exocytosis in β cells may play an important role in the maintenance of blood glucose concentration. First, the rate of insulin exocytosis triggered by glucose was relatively low (11 events $cell^{-1}$ min^{-1}) and the time course of secretion is relatively long, persisting for up to several minutes or hours. Thus, the suppression of sequential exocytosis prevents massive mobilization of insulin granules that would result in hypersecretion and in depletion of insulin. Second, the rarity of sequential exocytosis obliges β cells to transport insulin granules to the cell surface for exocytosis (Hisatomi et al., 1996; Rorsman and Renström, 2003). Such transportation, which is energy dependent, might act as a fuel sensor for insulin granule exocytosis (Takahashi et al., 1999; Kasai et al., 2002; Rorsman and Renström, 2003). Thus, the suppression of sequential exocytosis in β cells may be an important aspect of the secretory physiology of these cells.

Materials and methods

Isolation of mouse pancreatic islets

Pancreatic islets were isolated from 8- to 12-week-old ICR mice by collagenase digestion and were maintained for 1–12 h under a humidified atmosphere of 5% CO_2 at 37°C in DME containing glucose (1.0 mg/ml) and supplemented with 10% FBS, 100 μU/ml penicillin, and 100 mg/ml streptomycin. The islets were transferred with a Pipetman (Gilson) to thin (0.1-mm) glass coverslips (Matsunami-glass) in the recording chamber. The standard external bathing solution (Sol A) contained 150 mM NaCl, 5 mM KCl, 1 mM $MgCl_2$, 2 mM $CaCl_2$, 10 mM Hepes-NaOH, pH 7.4, and 2.8 mM glucose. Imaging experiments were performed within 20 min after placing an islet in Sol A containing 0.7 mM SRB (Molecular Probes). Forskolin (Sigma-Aldrich) or PMA (Sigma-Aldrich) was initially dissolved in DMSO at 10–50 mM and was subsequently diluted in Sol A. Methyl-β-cyclodextrin (Sigma-Aldrich) was directly dissolved in Sol A.

Two-photon excitation imaging

Two-photon excitation imaging of islets was performed with an inverted microscope (model IX70; Olympus) and a laser-scanning microscope (model FluoView; Olympus) equipped with a water-immersion objective lens (UplanApo60×W/IR; numerical aperture, 1.2). The laser power at the specimen was 3–10 mW, and two-photon excitation was effected at 830 nm, with images acquired every 0.3–2 s. The fluorescence of SRB, of fura-2 and fura-2FF, and of ECFP was measured at 550–650 nm, 400–530 nm, and 400–490 nm, respectively. In ECFP measurement, laser power and photomultiplier voltage were set to 8 W and 500 V, respectively. 12-bit images were color-coded with autumn color codes of FluoView. All experimental procedures were performed under yellow light illumination (FL40S-Y-F; National) to prevent unintended photolysis of the caged-Ca^{2+} compound (see the following section). Most experiments were performed at RT (24–25°C), although the temperature of the bathing solution was increased to 33–35°C with a heater (Daia Medical System) in some experiments.

Exocytic events were counted in a region of interest (ROI) with an area of 3,000–5,000 μm^2 and were normalized to an area of 2,000 μm^2. Given that the thickness of the optical section (T) in our setup is ∼0.8 μm, the volume of the normalized ROI is 1,600 μm^3. We expressed the number of events in the normalized ROI as events per cell, given that the volume of individual β cells is ∼1,600 (β cells have a mean diameter of 14.0 μm and constitute 90% of cells in an islet, or one β cell/1,596 μm^3 of an islet). For example, a frequency of 11.2 (or 45) events per cell per minute can also be expressed as 0.018 (or 0.073) events per square micrometer of plasma membrane per minute (a). In this example, the mean frequency of events (λ) within 1 min and a distance of <0.5 μm ($2b$) is predicted to be between πab^2 and

$$\pi ab\sqrt{b^2 + (T/2)^2},$$

considering the slope of the plasma membrane relative to the focal plane. Then, the proportion of random simultaneous events is estimated as

$$\left(\frac{1}{2}\lambda^2\right)/\lambda = 0.18\text{–}0.33\%$$

(or 0.72–1.3%) based on Poisson statistics. Peak fluorescence intensities of individual exocytic events were converted to the diameters ($2r$) of granules with the equation

$$\frac{4}{3}\pi r^3 = \frac{F_{SG}T}{F_S},$$

where F_{SG} and F_S represent the fluorescence of SRB in a single granule and in solution (with an area of 1 μm^2), respectively.

Photolysis of a caged-Ca^{2+} compound

The acetoxymethyl esters (AMs) of the Ca^{2+} indicators, fura-2 (Molecular Probes) and fura-2FF (Tef Lab), as well as that of the caged-Ca^{2+} compound NP-EGTA (Molecular Probes) were dissolved in DMSO at a high concentration (2–10 mM). Islets were loaded with these compounds by incubation for 30 min at 37°C in serum-free DME containing 10 μM fura-2-AM (or fura-2FF-AM), 25 μM NP-EGTA-AM, 0.03% cremphor EL (Molecular Probes), and 0.1% BSA, and were washed with Sol A. Photolysis of NP-EGTA was induced with a brief flash (0.2–0.5 s) of a mercury lamp (model IX-RFC; Olympus). The resulting increase in $[Ca^{2+}]_i$ was monitored by the

decrease in fluorescence intensity of fura-2FF (excitation wavelength: 830 nm) and was calculated as

$$K_d \frac{1 - F/F_{max}}{F/F_{max} - F_{min}/F_{max}},$$

where K_d, F_{max}, and F_{min} represent the dissociation constant for the interaction between fura-2FF and Ca^{2+} and the maximal and minimal fluorescence intensities, respectively. Calibration of fura-2FF was performed in vivo by exposing islets to Sol A containing 10 μM 4-bromo-A23187 (free acid; Molecular Probes), 30 μM cyclopiazonic acid (Sigma-Aldrich), and free $CaCl_2$ concentrations of 10 mM, 63 μM, or 0; the solution containing 63 μM free Ca^{2+} was prepared as described previously (Neher, 1988). In our islet preparations, the resting fluorescence was the same as F_{max}; we estimated F_{min}/F_{max} to be 0.1, and K_d is 31 μM.

Adenoviral infection

The mouse cDNA encoding SNAP25b was amplified by PCR with the forward primer 5′-GCGAATTCAATGGCCGAGGACGCAG-3′ and the reverse primer 5′-CGGTCGACTTAACCACTTCCCAGCATC-3′, which incorporate SalI and EcoRI sites at the 5′ and 3′ ends of the SNAP25 cDNA sequence, respectively. The PCR product was digested with SalI and EcoRI and inserted into the corresponding sites of the expression vector pECFP-C1 (CLONTECH Laboratories, Inc.), yielding a vector that encodes a fusion protein in which ECFP is attached to the NH_2 terminus of SNAP25 (Wei et al., 2000). An adenoviral vector that encodes the ECFP-SNAP25 fusion protein was constructed as described previously (Miyake et al., 1996). Islets were infected with the adenoviral vector (7×10^7 plaque-forming units per milliliter) for 2 h in serum-free culture medium, washed, and incubated for an additional 10–18 h before experiments.

Online supplemental material

Online supplemental material shows a video of the real-time image shown in Fig. 1 B. Online supplemental material is available at http://www.jcb.org/cgi/content/full/jcb.200312033/DC1.

We thank T. Kise and N. Takahashi for technical assistance.

This work was supported by Grants-in-Aid from the Ministry of Education, Culture, Sports, Science and Technology of Japan and from the Japan Society for the Promotion of Science, as well as by research grants from the Human Frontier Science Program Organization, Yamanouchi Foundation for Research on Metabolic Disorders, and Japan Diabetes Foundation.

Submitted: 3 December 2003
Accepted: 23 March 2004

References

Alvarez de Toledo, G., and J.M. Fernandez. 1990. Compound versus multigranular exocytosis in peritoneal mast cells. *J. Gen. Physiol.* 95:397–409.

Bekkers, J.M., G.B. Richerson, and C.F. Stevens. 1990. Origin of variability in quantal size in cultured hippocampal neurons and hippocampal slices. *Proc. Natl. Acad. Sci. USA.* 87:5359–5362.

Bokvist, K., L. Eliasson, C. Ämmälä, E. Renström, and P. Rorsman. 1995. Co-localization of L-type Ca^{2+} channels and insulin-containing secretory granules and its significance for the initiation of exocytosis in mouse pancreatic B-cells. *EMBO J.* 14:50–57.

Bokvist, K., M. Holmqvist, J. Gromada, and P. Rorsman. 2000. Compound exocytosis in voltage-clamped mouse pancreatic beta-cells revealed by carbon fibre amperometry. *Pflugers Arch.* 439:634–645.

Chamberlain, L.H., R.D. Burgoyne, and G.W. Gould. 2001. SNARE proteins are highly enriched in lipid rafts in PC12 cells: implication for the spatial control of exocytosis. *Proc. Natl. Acad. Sci. USA.* 98:5619–5624.

Cochilla, A.J., J.K. Angleson, and W.J. Betz. 2000. Differential regulation of granule-to-granule and granule-to-plasma membrane fusion during secretion from rat pituitary lactotrophs. *J. Cell Biol.* 150:839–848.

Dean, P.M. 1973. Ultrastructural morphometry of the pancreatic b-cell. *Diabetologia.* 9:115–119.

Douglas, W.W. 1974. Involvement of calcium in exocytosis and the exocytosis–vesiculation sequence. *Biochem. Soc. Symp.* 39:1–28.

Dvorak, A.M., S.J. Galli, E. Morgan, A.S. Galli, M.E. Hammond, and H.F. Dvorak. 1981. Anaphylactic degranulation of guinea pig basophilic leukocytes. I. Fusion of granule membranes and cytoplasmic vesicles formation and resolution of degranulation sacs. *Lab. Invest.* 44:174–191.

Guo, Z., C. Turner, and D. Castle. 1998. Relocation of the t-SNARE SNAP-23 from lamellipodia-like cell surface projections regulates compound exocytosis in mast cells. *Cell.* 94:537–548.

Hafez, I., A. Stolpe, and M. Lindau. 2003. Compound exocytosis and cumulative fusion in eoxinophils. *J. Biol. Chem.* 278:44921–44928.

Hartmann, J., S. Scepek, I. Hafez, and M. Lindau. 2003. Differential regulation of exocytotic fusion and granule-granule fusion in eosinophils by Ca^{2+} and GTP analogs. *J. Biol. Chem.* 278:44929–44934.

Hisatomi, M., H. Hidaka, and I. Niki. 1996. Ca^{2+}/calmodulin and cyclic 3,5′ adenosine monophosphate control movement of secretory granules through protein phosphorylation/dephosphorylation in the pancreatic beta-cell. *Endocrinology.* 137:4644–4649.

Ichikawa, A. 1965. Fine structural changes in response to hormonal stimulation of the perfused canine pancrease. *J. Cell Biol.* 24:369–385.

Ito, K., Y. Miyashita, and H. Kasai. 1997. Micromolar and submicromolar Ca^{2+} spikes regulating distinct cellular functions in pancreatic acinar cells. *EMBO J.* 16:242–251.

Jacobsson, G., A.J. Bean, R.H. Scheller, L. Juntti-Berggren, J.T. Deeney, P.O. Berggren, and B. Meister. 1994. Identification of synaptic proteins and their isoform mRNAs in compartments of pancreatic endocrine cells. *Proc. Natl. Acad. Sci. USA.* 91:12487–12491.

Kasai, H., T. Suzuki, T.T. Liu, T. Kishimoto, and N. Takahashi. 2002. Fast and cAMP-sensitive mode of Ca^{2+}-dependent exocytosis in pancreatic beta-cells. *Diabetes.* 51(Suppl 1):S19–S24.

Lang, T., D. Bruns, D. Wenzel, D. Riedel, P. Holroyd, H. Thiele, and R. Jahn. 2001. SNAREs are concentrated in cholesterol-dependent clusters that define docking and fusion sites for exocytosis. *EMBO J.* 20:2202–2213.

Leung, Y.M., L. Sheu, E. Kwan, G. Wang, R. Tsushima, and H. Gaisano. 2002. Visualization of sequential exocytosis in rat pancreatic islet beta cells. *Biochem. Biophys. Res. Commun.* 292:980–986.

Miyake, S., M. Makimura, Y. Kanegae, S. Harada, Y. Sato, K. Takamori, C. Tokuda, and I. Saito. 1996. Efficient generation of recombinant adenoviruses using adenovirus DNA-terminal protein complex and a cosmid bearing the full-length virus genome. *Proc. Natl. Acad. Sci. USA.* 93:1320–1324.

Neher, E. 1988. The influence of intracellular calcium concentration on degranulation of dialysed mast cells from rat peritoneum. *J. Physiol.* 395:193–214.

Nemoto, T., R. Kimura, K. Ito, A. Tachikawa, Y. Miyashita, M. Iino, and H. Kasai. 2001. Sequential-replenishment mechanism of exocytosis in pancreatic acini. *Nat. Cell Biol.* 3:253–258.

Oheim, M., D. Loerke, R.H. Chow, and W. Stuhmer. 1999. Evanescent-wave microscopy: a new tool to gain insight into the control of transmitter release. *Philos. Trans. R. Soc. Lond. B Biol. Sci.* 354:307–318.

Orci, L., and W. Malaisse. 1980. Hypothesis: single and chain release of insulin secretory granules is related to anionic transport at exocytotic sites. *Diabetes.* 29:943–944.

Rohlich, P., P. Anderson, and B. Uvnas. 1971. Electron microscope observations on compounds 48–80–induced degranulation in rat mast cells. Evidence for sequential exocytosis of storage granules. *J. Cell Biol.* 51:465–483.

Rorsman, P., and E. Renström. 2003. Insulin granule dynamics in pancreatic beta cells. *Diabetologia.* 46:1029–1045.

Scepek, S., and M. Lindau. 1993. Focal exocytosis by eosinophils–compound exocytosis and cumulative fusion. *EMBO J.* 12:1811–1817.

Tai, P.C., and C.J. Spry. 1981. The mechanisms which produce vacuolated and degranulated eosinophils. *Br. J. Haematol.* 49:219–226.

Takahashi, N., T. Kadowaki, Y. Yazaki, Y. Miyashita, and H. Kasai. 1997. Multiple exocytotic pathways in pancreatic β cells. *J. Cell Biol.* 138:55–64.

Takahashi, N., T. Kadowaki, Y. Yazaki, G.C. Ellis-Davies, Y. Miyashita, and H. Kasai. 1999. Post-priming actions of ATP on Ca^{2+}-dependent exocytosis in pancreatic beta cells. *Proc. Natl. Acad. Sci. USA.* 96:760–765.

Takahashi, N., T. Kishimoto, T. Nemoto, T. Kadowaki, and H. Kasai. 2002. Fusion pore dynamics and insulin granule exocytosis in the pancreatic islet. *Science.* 297:1349–1352.

Wei, S., T. Xu, U. Ashery, A. Kollewe, U. Matti, W. Antonin, J. Rettig, and E. Neher. 2000. Exocytotic mechanism studied by truncated and zero layer mutants of the C-terminus of SNAP-25. *EMBO J.* 19:1279–1289.

Zenisek, D., J.A. Steyer, M.E. Feldman, and W. Almers. 2002. A membrane marker leaves synaptic vesicles in milliseconds after exocytosis in retinal bipolar cells. *Neuron.* 35:1085–1097.